Available online at www.sciencedirect.com
SCIENCE DIRECT®
Scripta Materialia 51 (2004) 915–920
Scripta MATERIALIA
www.actamat-journals.com

Experimental study on the thermal stability of Cr filaments in a Cu–Cr–Ag in situ composite

D. Raabe [a,*], J. Ge [b]

[a] Max-Planck-Institut für Eisenforschung, Max-Planck-Str. 1, 40237 Düsseldorf, Germany
[b] Dalian Railway Institute, 116028 Dalian, PR China

Received 9 October 2003; received in revised form 22 May 2004; accepted 17 June 2004
Available online 23 July 2004

Abstract

We investigate Cr filaments in heavily drawn Cu–10 wt.%Cr–3 wt.%Ag in situ composite wires as a function of temperature and time. The filaments undergo a capillarity-driven shape change from a bamboo morphology with grain boundary grooves to complete spherodization. We interpret the results in terms of analytical models.

Keywords: Metal matrix composites; Drawing; Interface diffusion; Coarsening; Magnet design

1. Introduction

Owing to their excellent strength and good resistive conductivity Cu-based in situ composites play a key role for the manufacturing of high mechanically stressed electrical devices. Prominent examples are in the areas of high field capacitor driven pulsed or steady state Bitter-type direct current magnet design, robotics, cables, and electrical contacts [1–3]. While in the past, much attention was placed on binary alloys consisting of Cu and a body centered cubic (bcc) metal [4–12] or Cu and Ag [13–17], less efforts were made to widen the spectrum of in situ metal–matrix composites towards ternary Cu-based alloys.

Some recent investigations have aimed to fill that gap. Morris and Joyce [18] worked on hypereutectic Cu–2 wt.% Cr–0.3 wt.% Zr alloys, Verhoeven et al. [3] on Cu–15 wt.% Nb–2 wt.% Ag alloys, Troxel [19] on dispersoid-strengthened Cu–10 wt.% Nb–(0.3→1.1) wt.% Al_2O_3 alloys, Fritzemeier [20] on Cu–15 wt.% Nb–2 wt.% Ag alloys, Spitzig et al. [21] on Cu–20 wt.% Nb–7 wt.% Ag alloys, Spaic and Pristavec [22] on Cu–(1→7) wt.% Ag–0.3 wt.% Zr alloys, Raabe and Mattissen [23–25] on Cu–4 wt.% Nb–8.2 wt.% Ag alloys, and Miyake et al. [26,27] on Cu–(4.5→10) wt.% Cr–(13→3) wt.% Ag.

The basic strategy in ternary alloy development lies in exploiting filamentary Hall–Petch-type as well as age hardening at the same time. Both effects are due to the interaction of mostly incoherent heterophase interfaces with lattice dislocations. This means that the physics of hardening in ternary alloys has the same origin as in binary alloys. However, adding a third chemical element allows for a larger variety of possible kinetical paths for attaining a well tailored flow stress-conductivity profile.

During operation in magnets, the composites undergo resistive heating. This effect may entail microstructural changes leading to a degradation of the composite properties. Designing magnets for prolonged service, therefore, requires better knowledge about the

* Corresponding author. Tel.: +49 211 679 2278; fax: +49 211 679 2333.
E-mail address: raabe@mpie.de (D. Raabe).

1359-6462/$ - see front matter
doi:10.1016/j.scriptamat.2004.06.016

microscopic thermal stability and the resulting macroscopic property changes of the materials.

The most significant effect observed in Cu- and Ag-based metal–matrix composites upon heat treatment is the capillarity-driven shape change of the filaments. The microstructural changes are characterized by the formation of a bamboo-type morphology followed by fiber break-up, spherodization, and coarsening. This topological evolution was described in a number of articles [28–34]. It was also observed in these studies that the described steps did not happen in strict consecutive order but occurred in part simultaneously. This means that different stages of coarsening were found in different parts of the same sample due to the size distributions of the filaments and the overlap of the diffusion fields.

A detailed investigation and understanding of the described shape changes is of relevance for two reasons. First, the strength of such in situ composites is to a large extent governed by the spacing of the heterophase interfaces following a modified Hall–Petch-type relationship [4–11]. Therefore, one may expect that filament break-up and coarsening leads to a drop in flow stress. Second, a more fundamental interest of this study lies in elucidating the kinetics of the observed morphological changes.

2. Experimental procedure

The Cu–10 wt.% Cr–3 wt.% Ag alloy used in this study was melted in a vacuum induction furnace. The ingredients were electrolytic Cu, Cr with 99.99 wt.% purity, and Ag with 99.9 wt.% purity. The alloy was cast into a Cu mould at 1570 K. From the as-cast sample, cylindrical ingots of 18 mm diameter were cut. Samples were produced by rotary swaging and wire drawing. The final total strain amounted to $\eta = 3.95$ ($\eta = \ln(A_0/A)$, A: wire cross-section (98% engineering cross-sectional reduction)). After plastic straining the samples were vacuum annealed at different temperatures. Further processing details are in [26,27].

The resulting microstructures were examined using optical microscopy and scanning electron microscopy (SEM). For optical investigation, the samples were ground and etched using a solution of 50 ml C_2H_5OH, 50 ml HF, and 30 ml HNO_3. This etching removed the smeared out Cr debris which had formed during grinding on the sample surface. The inter-filament spacing was determined by an edge-to-edge measurement. The morphology of the Cr dendrites and Cr fibers was measured using a selective etching, where the Cu–Ag matrix and the precipitated Ag were dissolved by dilute nitric acid. The experimental data of the break-up diameters were averaged from 50 measurements. The break-up diameter is defined as the filament diameter at which separation of grooved filaments occurs leading to the formation of chains which consist of disconnected portions of fiber material. This means that we measured at a given time and annealing temperature those diameters of filaments which were just on the verge of pinching off.

3. Experimental results

The as-cast samples contained Cr dendrites in a Cu–Ag matrix. The average diameter of the Cr particles in the as-cast state was about 5000 nm. The drawn specimens ($\eta \approx 3.95$) were characterized by elongated Cr filaments which formed from the dendrites. Further details of the microstructures before annealing are given in [26,27].

Fig. 1a–c presents SEM micrographs taken from transverse wire sections of the drawn Cu–10 wt.% Cr–3 wt.% Ag alloy at a total strain of $\eta = 3.95$ after different annealing times at 1273 K. Fig. 1a shows the microstructure after 33 min (1273 K), Fig. 1b after 60 min (1273 K), and Fig. 1c after 4 h (1273 K).

Fig. 2a–c shows longitudinal sections which document the transition from a fiber type to a bamboo-type morphology during annealing.

The transverse micrographs in Fig. 1 reveal that the initially heavily curled cross-sectional shapes of the Cr filaments undergo shape changes which are characterized by the transition to a more cylindrical shape, followed by competitive coarsening (e.g. Fig. 1c). The longitudinal sections reveal that neighboring portions in the elongated Cr filaments separate by the formation of grooves, by the subsequent separation of the grooved portions into a chain-line arrangement, and by the spherodization and competitive ripening of these parts (see also [27]).

Besides the morphological changes of the Cr filaments, coarsening of the matrix grains due to normal grain growth was also observed. Furthermore, it is an important detail that the break-up of the filaments during annealing often coincides with the location of large angle grain boundaries of the matrix grains.

4. Discussion

The break-up and coarsening of metal filaments embedded in a metal matrix occurring during annealing were already the subject of previous investigations [28–34]. Malzahn-Kampe et al. [28,29] were the first to show in their work on the thermal stability of Fe plates in Cu–Fe in situ composites that the mechanisms which induce morphological changes in rod- or plate-shaped microstructures embedded in a Cu matrix and exposed to elevated temperature are driven by capillary forces. The basic starting point for an analysis of this phenomenon,

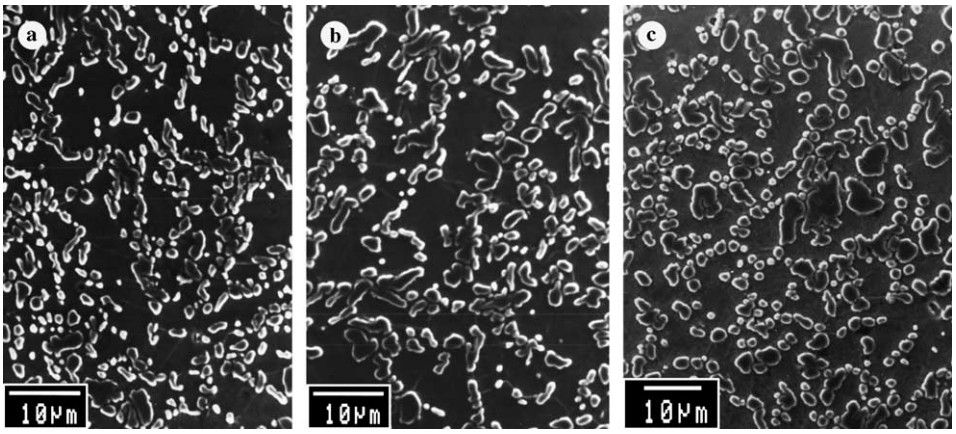

Fig. 1. SEM micrographs taken from transverse wire sections of the drawn Cu–10 wt.% Cr–3 wt.% Ag alloy at a total strain of $\eta = 3.95$ after different annealing times at 1273 K. (a) Microstructure after 33 min; (b) after 60 min; (c) after 4 h.

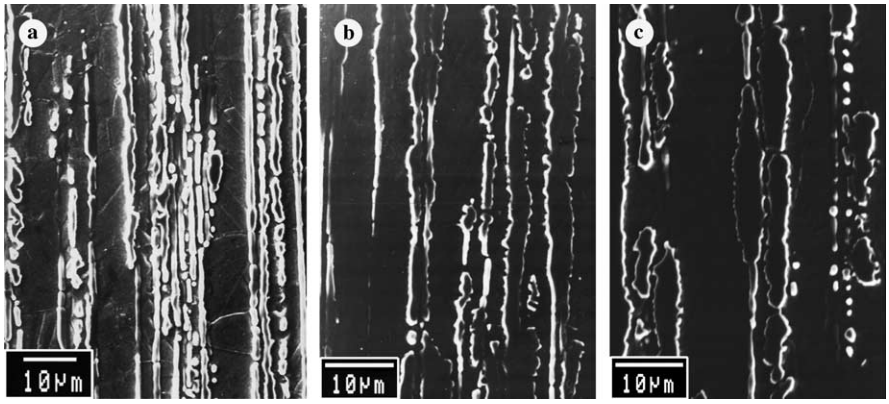

Fig. 2. SEM micrographs taken from longitudinal wire sections of the drawn Cu–10 wt.% Cr–3 wt.% Ag alloy at a total strain of $\eta = 3.95$ after different annealing times at 1273 K. (a) Microstructure after 33 min; (b) after 60 min; (c) after 4 h.

therefore, is the mechanism of curvature-induced surface diffusion [35] which is captured by the Gibbs–Thomson equation which relates differences in the chemical potential to the local curvature of an interface

$$\Delta\mu = \Omega K \gamma_s \tag{1}$$

where $\Delta\mu$ is the difference in chemical potential of an atom on a curved surface relative to one on a flat surface, Ω the volume of diffusing atoms, K the difference in local surface curvature between two surfaces, and γ_s the surface energy.

The growth of a shape perturbation on a cylinder shaped phase was analyzed already more than a century ago by Rayleigh [36]. Nichols and Mullins [35], Cline [37], and Weatherly [38] have applied Rayleigh's perturbation approach which was originally formulated for a liquid cylinder to solid shapes. Their linear stability analysis shows that if interfacial diffusion controls the perturbation process, the rate of growth of a sinusoidal disturbance in an infinite cylinder will be given by

$$\frac{d\delta}{d\tau} = \delta B \omega^2 \left(\frac{1}{r_0^2} - \omega^2\right) \tag{2}$$

where δ is the perturbation amplitude, τ the annealing time; $\omega = 2\pi/\lambda$ the spatial frequency of the perturbation, λ the wavelength of the perturbation, and r_0 the initial radius of the cylinder. The coefficient B amounts to

$$B = \frac{D_I \gamma_I \Omega^2}{k_B T} \tag{3}$$

where D_I is the diffusion coefficient for the atomic species of the filament in the filament/matrix interface, γ_I the filament/matrix interfacial energy, Ω the atomic volume of the diffusing species, k_B the Boltzmann constant, and T the absolute temperature. Solving this equation gives the time required for the filaments with an initial radius r_0 to break up

$$\tau = \frac{\ln\left(\frac{\delta}{\delta_0}\right)}{\left[\frac{D_I \gamma_I \Omega^2}{k_B T} \omega^2 \left(\frac{1}{r_0^2} - \omega^2\right)\right]} = \frac{\ln\left(\frac{r_0}{\delta_0}\right)}{[B(T) C(r_0, \lambda)]} \tag{4}$$

where

$$C(r_0,\lambda)=\omega^2\left(\frac{1}{r_0^2}-\omega^2\right) \tag{5}$$

and δ_0 is the initial sinusoidal perturbation on the surface of the filament or more precisely, in the filament/matrix interface. The value of δ_0 can be taken of the order of the Burgers vector. The initial radius of the filament r_0 is obviously the upper bound for the break-up process. The basic physical picture behind this Rayleigh-type instability approach is the assumption of critical perturbations occurring naturally in the plastically strained filament/matrix interface and their subsequent amplification due to capillarity-driven interface diffusion.

Mullins [39] and Ho and Weatherly [40] gave a more precise picture of such coarsening processes by describing the incipient stage in the diffusional separation of an elongated filament in terms of a thermal groove model. They assumed that if an array of internal grain boundaries is introduced into a cylinder- or plate-like microstructure, an initial local mechanical equilibrium of surface tension will be established at each of the triple point junctions and form a grain boundary groove. This effect leads to curvature of the interfaces which in turn entails gradients in the chemical potential. Diffusion of atoms leaving the curved groove in response to the chemical potential gradient will force the groove to grow and finally cause a plate or cylinder to separate. According to these works the annealing time, τ, required for the impingement of opposite thermal grooves amounts to

$$\tau=\left(\frac{r_0}{0.974Bm}\right)^4 \tag{6}$$

in case that interfacial diffusion prevails. In this equation, r_0 is the initial radius of the filament, m the tangent slope of the interface at the groove root which can be approximated by $\gamma_b/2\gamma_s$ where γ_b and γ_s are the grain boundary and surface energies, respectively, and B as defined in Eq. (3) [39].

A modification of this thermal groove model was suggested by Courtney and Malzahn-Kampe [29]. By using appropriate geometrical boundary conditions on volume transport, diffusion area and length, and curvature enabled them to describe the temporal evolution of the thickness fluctuations according to

$$\frac{\tau t}{\tau_b d}=\left\{\left[\frac{\cos(\phi)}{(1-\sin(\phi))^2}\right]\left[1-\frac{1}{2}\sin(\phi)-\left(\frac{\pi}{2}-\phi\right)\frac{1}{2\cos(\phi)}\right]\right\}\left(\frac{\pi}{2}-\phi\right)\frac{1}{64\sin(\phi)^2} \tag{7}$$

where t is the interface thickness over which interfacial diffusion occurs, d the plate thickness, $\phi=\cos^{-1}(\gamma_b/2\gamma_s)$, and τ_b a reference time, which can be approximated by

$$\tau_b=\frac{(d^3k_BT)}{Dc_0\gamma_s\Omega^2} \tag{8}$$

where c_0 is the equilibrium matrix concentration of filament material for a flat matrix/matrix interface.

For comparing the observed experimental data of break-up of the Cr filaments in the Cu–3 wt.% Ag matrix with these thermal groove models we used the following physical constants: For the diffusion of Cr in the Cu–3 wt.%Ag/Cr interface the surface diffusion coefficient was assumed as $D_s=1.1\times\exp(-52000/1.987T)$ cm^2/s [41], the interface energy for the heterophase Cr/CuAg boundary as $\gamma_s=2.3\times10^{-4}$ J cm^{-2} [3], the grain boundary energy for the Cr homophase boundaries as $\gamma_b=0.98\times10^{-4}$ J cm^{-2} [3], the tangent slope of the interface at the groove root $m=0.213$, the atomic volume $\Omega=0.8158\times10^{-23}$ cm^3, and an initial sinusoidal perturbation of $\delta_0=0.001\times r_0$ [42].

It must be underlined in this context that we use for the comparison with analytical theory only *average* values of the break-up diameters. Such procedure naturally includes two basic simplifications. First, the filament diameters and, therefore, also the break-up diameters are size *distributions*, but they are not sharp values. This means that the smallest diameter filaments will undergo capillary driven break-up along large energy grain boundaries long before those which have a large initial diameter and low energy internal grain boundaries. Second, it may be assumed that the kinetics observed is altered by the overlap of neighboring diffusion areas, i.e. the assumption of an infinite matrix surrounding the break-up zone is usually not justified.

Fig. 3 shows the predictions of the three models (assuming interfacial diffusion) together with the experimental data for the break-up diameters at 1029 and 1108 K as a function of time. All three models reveal the same slopes as a function of the annealing time, but they show different absolute values for the break-up diameters. The slope confirms that interfacial diffusion can be regarded as the controlling mechanism of break-up kinetics of the Cr filaments. The discrepancy in absolute numbers between the experimentally observed break-up diameters and those predicted by the models may be attributed to an incorrect value of the interface diffusion coefficient and to the influence of microstructure variation as mentioned above.

Another point often neglected in this context is the possibility of a considerable deviation of the mutual bulk solubilities of two sorts of atoms (such as Cu–Nb or Cu–Cr) from their respective equilibrium values in heavily in situ drawn specimens. For instance, Sauvage et al. [43] have documented large deviations from the mutual (negligible) equilibrium solubility of Cu and Nb within each other in the vicinity of Cu–Nb interfaces by using the 3D atom probe technique. Similar observations were made by Ohsaki et al. [44] for the Cu–Ag sys-

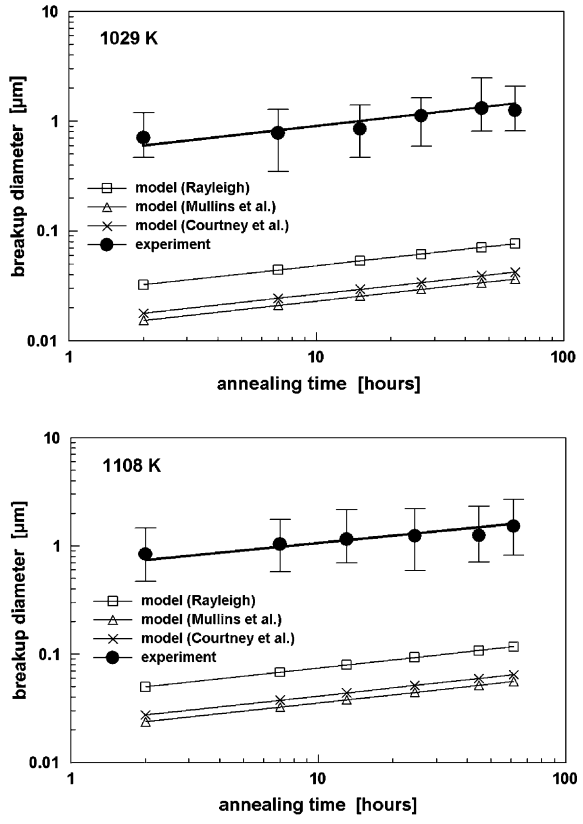

Fig. 3. Comparison of the predicted and experimental data of the break-up diameters as a function of time for 1029 and 1108 K.

tem. Hono [45] has recently observed similar effects at the Cu–Nb interfaces in heavily in situ drawn ternary Cu–8.2 wt.% Ag–4 wt.% Nb composite wires in a series of 3D atom probe measurements.

These various high-resolution observations show that a considerable percentage of excess atoms (probably up to 15 at.%) must be taken into account at the incoherent interfaces in heavily deformed Cu–Nb in situ composites.

We assume that similar non-equilibrium solubility effects such as those reported for the Cu–Nb system must be also considered in the Cu–Cr system which is of interest in this study. In thermal equilibrium these two sorts of atoms have only small mutual solubility which drops to near zero at room temperature. Maximum solubility of Cr in Cu amounts 0.89 at.% (0.71 wt.%) at 1350 K.

Such chemical deviations from the equilibrium data (which are assumed in the model calculations) might explain that also non-equilibrium bulk diffusion of atoms which were brought into solution during the heavy straining in addition to interface diffusion might play a significant role for the break-up kinetics explaining the observed deviations between the models and our experimental data. This would also favor the assumption that an increase in the total wire strain would systematically accelerate the thermally induced break-up kinetics due to bulk over-saturation and a corresponding enhanced diffusion flux. We can, however, not confirm this tendency from our data since the experiments reported here were essentially conducted on wires drawn to a strain of $\eta = 3.95$. Break-up kinetics of samples deformed to smaller strains were not systematically investigated in this study.

One important question in this context is the actual mechanism which leads to the increase in the observed mutual solubility. One effect might be the plastic co-deformation of the originally separated phases which, most likely, involves the transition of lattice dislocations from one phase into the other. This mechanisms has long been discussed as an important contribution to explain the plastic compatibility of the strained phases and the observed ductility of heavily wire drawn Cu-bcc or Cu-fcc alloys. Such penetration of lattice dislocations from one phase to another has two important consequences in the context of the current discussion. First, each transition of a dislocation across an incoherent heterophase interface requires the generation of secondary interface dislocations with a very small misfit vector. It is still unclear though whether these secondary dislocations alter/relax the interface structure and/or lead to secondary dislocation networks in front of those interfaces. Second, each transition of a lattice burgers vector through a heterophase interface transports material from one phase into the other by ordinary lattice translation (neglecting the secondary interface dislocations for a moment) promoting mechanically driven enhanced mutual solubility. Thermodynamic stabilization of such a non-equilibrium content of solved atoms might be due to the large capillary pressure inherent in such microstructures owing to the huge interface curvature of the coexisting phases.

5. Conclusions

We studied the break-up of Cr filaments in heavily drawn Cu–10 wt.% Cr–3 wt.% Ag in situ composite wires as a function of temperature and annealing time. The filaments revealed a curvature-driven shape change which was characterized by the gradual formation of a bamboo-type morphology where neighboring portions of the same filament became increasingly separated by growing thermal grooves. The kinetics of the process were compared to analytical models. The results suggested that the observed break-up kinetics can be interpreted in terms of a capillary driven process which is dominantly controlled by interface diffusion.

References

[1] Schneider-Muntau HJ. IEEE Trans Magnetics 1982;18:32.
[2] Embury JD, Hill MA, Spitzig WA, Sakai Y. MRS Bull 1993;8:57.

[3] Verhoeven JD, Spitzig WA, Jones LL, Downing HL, Trybus CL, Gibson ED, et al. J Mater Eng 1990;12:127.
[4] Bevk J, Harbison JP, Bell JL. J Appl Phys 1978;49:6031.
[5] Funkenbusch PD, Courtney TH. Acta Metall 1985;33:913.
[6] Spitzig WA, Pelton AR, Laabs FC. Acta Metall 1987;35:2427.
[7] Verhoeven JD, Spitzig WA, Schmidt FA, Krotz PD, Gibson ED. J Mater Sci 1989;24:1015.
[8] Raabe D, Heringhaus F, Hangen U, Gottstein G. Z Metallk 1995;86:405.
[9] Heringhaus F, Raabe D, Gottstein G. Acta Metall 1995;43:1467.
[10] Raabe D, Hangen U. Acta Metall 1996;44:953.
[11] Wood JT, Embury JD, Ashby MF. Acta Mater 1997;45:1099.
[12] Ellis TW, Kim ST, Verhoeven JD. J Mater Eng Perform 1995;4:581.
[13] Cline HE, Lee D. Acta Metall 1970;18:315.
[14] Frommeyer G, Wassermann G. Acta Metall 1975;23:1353.
[15] Sakai Y, Inoue K, Asano T, Maeda H. J Jpn Inst Metals 1991;55:1382.
[16] Asano T, Sakai Y, Oshikiri M, Inoue K, Maeda H, Heremans G, et al. Physica B: Condens Matter 1994;201:556.
[17] Sakai Y, Schneider-Muntau HJ. Acta Metall 1997;45:1017.
[18] Morris MA, Joyce JC. Acta Metall 1995;43:69.
[19] Troxel J. Adv Mater Proc 1995;147:35.
[20] Fritzemeier LG. Nanostruct Mater 1992;1:257.
[21] Spitzig WA, Wheelock PB, Ellis TW, Laabs FC. In: Micromechanics of advanced materials. Cleveland, OH: TMS Minerals Metals Materials Society; 1996. p. 341.
[22] Spaic S, Pristavec M. Metall 1996;4:254.
[23] Raabe D, Mattissen D. Acta Mater 1998;46:5973.
[24] Raabe D, Mattissen D. Acta Mater 1999;47:769.
[25] Mattissen D, Raabe D, Heringhaus F. Acta Mater 1999;47:1627.
[26] Miyake K, Hanzawa N, Takahara H, Kobayashi S, Raabe D. Jpn J Appl Phys 2000;39:119.
[27] Raabe D, Miyake K, Takahara H. Mater Sci Eng 2000;A291:186.
[28] Malzahn-Kampe JC, Courtney TH, Leng Y. Acta Metall 1989;37:1735.
[29] Courtney TH, Malzahn-Kampe JC. Acta Metall 1989;37:1747.
[30] Biner SB, Spitzig WA. Mater Sci Eng 1992;A150:213.
[31] Hardwick DA, Rhodes CG, Fritzemeier LG. Metall Trans 1993;24A:27.
[32] Hong SI, Hill MA, Sakai Y, Wood JT, Embury JD. Acta Metall 1995;43:3313.
[33] Sandim MJR, Shigue CY, Ribeiro LG, Filgueira M, Sandim HRZ. IEEE Trans Appl Supercond 2002;12:1195.
[34] Sandim MJR, Sandim HRZ, Shigue CY, Filgueira M, Ghivelder L. Supercond Sci Technol 2003;16:307.
[35] Nichols FA, Mullins WW. Trans Met Soc AIME 1965;233:1840.
[36] Rayleigh JWS. Proc London Math Soc 1880;11:57.
[37] Cline HE. Acta Metall 1971;19:481.
[38] Weatherly GC. Treat Mater Sci Technol 1975;8:121.
[39] Mullins WW. Trans Met Soc AIME 1960;218:354.
[40] Ho E, Weatherly GC. Acta Metall 1975;23:1451.
[41] Spitzig WA. Acta Metall 1991;39:1085.
[42] Pantsyrnyi VI, Shikov AK, Nikulin AD, Vorob'ova AE, Dergunova EA, Silaev AG, et al. IEEE Trans Magn 1996;32:2866.
[43] Sauvage X, Renaud L, Deconihout B, Blavette D, Ping DH, Hono K. Acta Mater 2001;49:389.
[44] Ohsaki S, Yamazaki K, Hono K. Scripta Mater 2003;48:1569.
[45] Hono K. Private communication on unpublished 3D atom-probe data taken on heavily in-situ drawn Cu–8.2 weight% Ag–4 weight% Nb composite wires, 2004.